JOURNAL OF MATERIALS SCIENCE 26 (1991) 3386–3391

Kinetics of secondary carbide precipitation in boron-modified cobalt alloys of MAR–M509 type

Z. OPIEKUN
Institute of Mechanical Engineering, Technical University in Rzeszów, Wincentego Pola 2, 35–959 Rzeszów, Poland

The effect of boron addition, introduced in different amounts (0.01, 1.48%) in heat-resistant cobalt-casting alloys of the MAR–M509 type, on the kinetics of precipitation of secondary carbides $Cr_{23}C_6$ is investigated during annealing at 975 °C for 21 h. Structure analysis of cobalt alloys tested in the as-cast condition and after annealing is also presented. It has been found that boron significantly shortens the incubation time for forming nuclei carbides of $Cr_{23}C_6$. Boron at 0.09% causes size reduction of primary phases, whereas higher boron additions create additional boride phases of the MB type of high tungsten content. Dilatometer curves for the precipitation of secondary carbides $Cr_{23}C_6$ in cobalt alloys of the MAR–M509 type have been described using Wert's empirical equation, $W_t = kt^n$.

1. Introduction

Heat-resistant cobalt alloys are frequently composed of so-called γ carbide-strengthened cobalt austenite. Apart from carbides there can be other phases such as geometrically close-packed (GCP)-γ (Ni, Co)$_3$(Al, Ti), ηNi_3Ti; topologically close-packed (TCP)-σ(Co, Ni) (Cr, Mo, W), Laves Co_2Ta, μCo_7W_6, R(rhombohedr.) (Co, Cr, W, Fe), π(Co, Ni, Cr, W), C; nitrides (Ta, Ti, Zr) (C, N) and Ni_5Zr [1]. In the process of alloy casting these are the primary phases precipitated. However, as a result of annealing, or during the work at increased temperatures, secondary dispersion hardening phases, mostly carbides $Cr_{23}C_6$, are precipitated from the austenite matrix of cobalt base alloys [2–9].

Boron is a particular component of cobalt alloys. According to Stickler [1] its content in such alloys amounts to 0.0–0.1 wt.%, but there is also a cobalt-base alloy known to contain about 4.0 wt % B [10]. Boron shows a segregation tendency on the grain boundaries, thus reducing their energy and therefore improving their heat-resistant properties. For example the cobalt-base alloy of HS–25 has a creep strength of 70 MPa, 10.3×10^3 p.s.i. (1000 h, 900 °C), and with about 0.01% B its creep strength is 95 MPa, 13.7 $\times 10^3$ p.s.i. (1000 h, 900 °C). It also influences the size reduction of primary phases and morphology changes in the heat-treatment process, as well as the course of the precipitation process of the secondary phases when the alloys are utilized.

Moreover, borides retain their crystallographic orientation with the alloy matrix and are pliant to plastic strain which, combined with their great resistance to oxidation, determines the simultaneous increase in creep resistance and plasticity of their alloys [11].

This paper discusses the influence of different boron additions into MAR–M509-type alloys on the kinetics of the precipitation of secondary carbides, $Cr_{23}C_6$, in their matrices.

2. Experimental procedure

Cobalt-base alloys of the MAR–M509 type containing boron were obtained from pure alloying components in an induction crucible furnace type (type Asec-15) and an alundum crucible, and cast in investment moulds. The MAR–M509-type alloy was selected for the investigations because it is characterized by the longest time of rupture during tests for high-temperature creep [2].

The chemical composition of this alloy was as follows (wt%): 23.62 Cr, 9.40 Ni, 7.0 W, 1.86 Ta, 0.20 Ti, 1.68 Zr, 0.71 C. Five alloys of different boron content were received on the basis of this fundamental chemical composition. Alloy No. 1 was cast without boron content.

Amorphous boron (in the powdered form) of 97% purity was introduced into the alloys using die stamping. Die stamping was achieved by mixing boron powder with electrolytic nickel powder (50 wt % each) and pressing it in a die block. The die stampings were placed in a crucible among the pieces of graphite, cobalt, nickel, chromium and tungsten. By the end of melting process, tantalum and titanium were added directly, as well as zirconium as a Ni–Zr master alloy. The compositions of the cast alloys are given in Table I.

3. Results

Investigation of the precipitation kinetics of secondary carbides $Cr_{23}C_6$ in heat-resistant cobalt alloys with

0022–2461/91 $03.00 + .12

TABLE I Compositions of experimental alloys

Alloy	Compositions (wt %, balance cobalt)								
no.	Cr	Ni	W	Ta	Ti	Zr	B	C	S
1	24.33	10.15	6.70	2.67	0.15	1.47	–	0.71	0.0030
2	24.02	10.32	6.67	2.71	0.16	1.48	0.09	0.71	0.0029
3	24.30	10.60	6.62	2.70	0.18	1.53	0.47	0.69	0.0028
4	24.22	10.33	6.58	2.70	0.18	1.52	1.00	0.73	0.0030
5	24.20	10.05	6.82	2.68	0.17	1.49	1.48	0.71	0.0028

no boron content, and with different boron content, was carried out on specimens 4 mm in diameter and 30 mm in length, using an LS-4 type dilatometer with inductive sensor coupled with an x–y Ricken–Denski recorder. The specimens were isothermally annealed in a dilatometer furnace at a temperature of about 975 °C.

3.1. Microstructure

The structure of the alloys in the as-cast condition and after annealing was examined by optical microscopy and scanning electron microscopy (SEM) using metallographic specimens. The metallographic specimens were prepared by mechanical polishing and electrolytic etching in 50% aqueous HNO_3 solution at about 8 V.

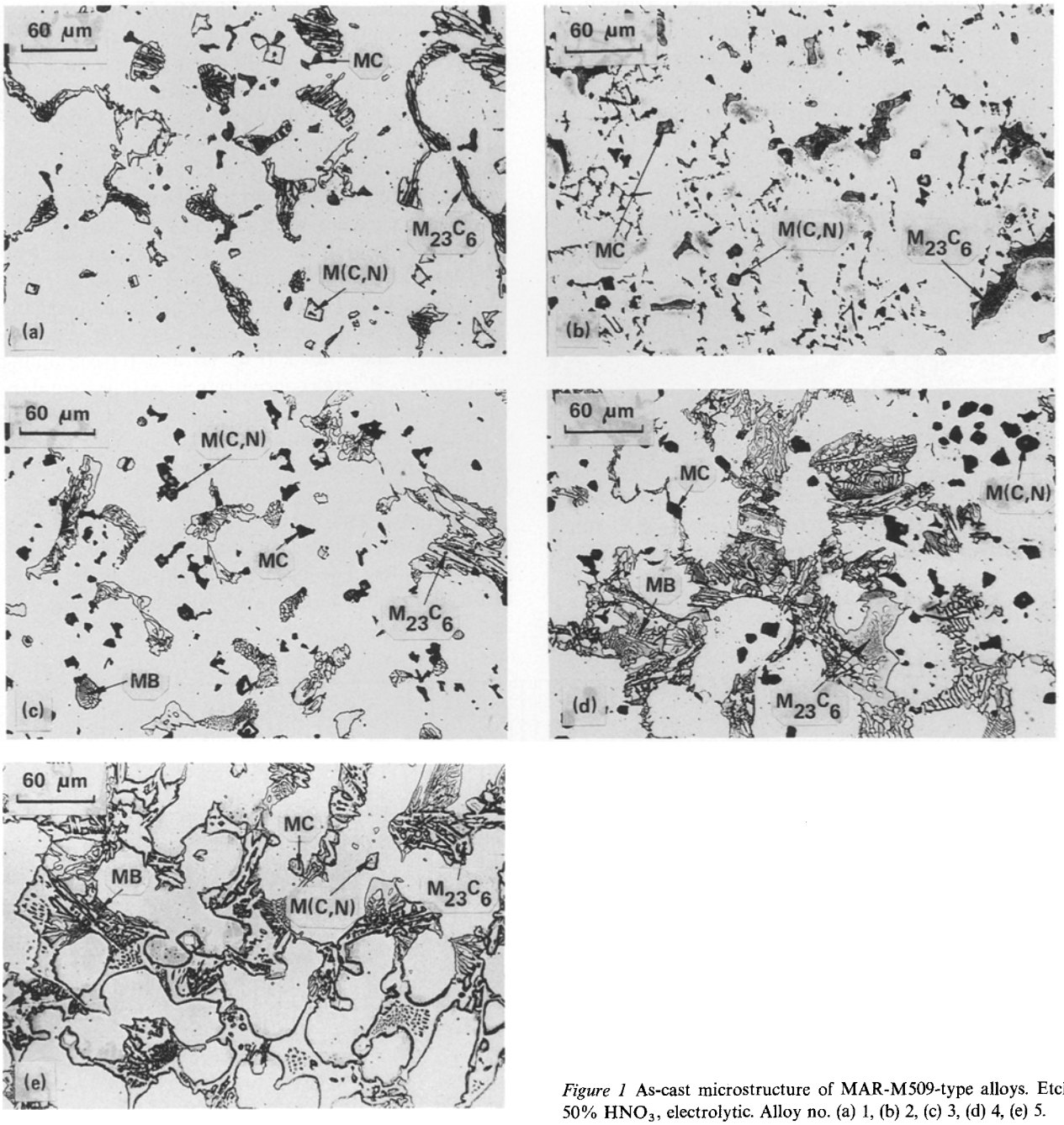

Figure 1 As-cast microstructure of MAR-M509-type alloys. Etch 50% HNO_3, electrolytic. Alloy no. (a) 1, (b) 2, (c) 3, (d) 4, (e) 5.

The structure of alloys in the as-cast condition is shown in Fig. 1. Better discrimination of the primary phases, with better contrast, was attained by using an electron beam Novascan 30 Type SEM (Carl Zeiss, West Germany). Fig. 2 shows the structure of alloy no. 4, observed using SEM.

To identify the boride phases present in alloys 3 to 5, an isolate was made from alloy no. 5. The phases were electrolytically extracted from this alloy using a solution of 90 cm^3 C_2H_5OH, 10 cm^3 HCl, tartaric acid (1 wt %), and an electric current of about 300 mA. The type of boride phase present in alloys 3 to 5 was identified by the Debye–Scherrer method with the use of CuK_α radiation.

An auxiliary energy device, "Kevex-Ray", coupled with SEM was used to define the alloying elements that appear in the composition of borides by the quantitative point method. Fig. 3 shows the characteristic radiation spectrum for boride phase with the peaks from tungsten, chromium and cobalt as observed on the spectrometer monitor.

When the structure of examined cobalt alloys in the as-cast condition is analysed (Figs 1 and 2) it is possible to observe additional boride phases of the MB type. They can be defined as (W, Cr, Co)B if boron additions are above 0.1%. However, tungsten is the main component of this boride (three peaks from tungsten, see Fig. 3). After 0.09% B is added to alloy no. 2, large and ramificated $M_{23}C_6$-type primary carbides of high chromium content (Fig. 1a) become smaller and disintegrated (Fig. 1b). No boride phase is observed in the microstructure of the alloy. MC-type primary carbides of high tantalum content, and M(C, N)-type carbonitrides of high zirconium content, are also crumbled.

In alloy no. 3 the increase of boron content to about 0.47% results in the appearance of borides in its structure as primary separated and concentrated precipitates (Fig. 1c). Carbides and carbonitrides in this alloy are similar in size to those in alloy no. 1 (with no boron content). Further increase in boron content of up to 1.00% in alloy no. 4 (Fig. 1d) and up to 1.48% B in alloy no. 5 (Fig. 1e) promotes the formation of a continuous net of borides and carbides of $M_{23}C_6$-type which crystallize together, around the matrix grains γ. Between these phases there are carbides of MC type and carbonitrides of M(C, N) type in the matrix. The boride phases, together with $M_{23}C_6$-type carbide, produce a continuous net in alloy no. 5 (Fig. 1e).

The microstructure of alloys 1 to 5 after annealing at 975 °C for 21 h in the dilatometer furnace are shown in Figs 4 and 5. Fig. 5 shows the structure of alloy no. 5 as observed with the use of SEM.

After annealing at 975 °C for 21 h in alloys 1 to 5, secondary $Cr_{23}C_6$ carbides precipitated in their matrices. Those carbides were identified on thin foils by electron diffraction and with transmission electron microscopy (TEM) [2]. In alloy no. 1 (Fig. 4a), $Cr_{23}C_6$ carbides are evenly precipitated in matrix γ during the annealing (ageing) process and tiny particles are formed. In alloy no. 2 (Fig. 4b and b′) containing about 0.09% B, large concentrations of tiny secondary $Cr_{23}C_6$ carbides are visible around primary $M_{23}C_6$ carbides. Moreover, in matrix γ of this alloy $Cr_{23}C_6$ carbides precipitate at {1 1 1} planes along characteristic lines.

In alloys 3 and 5 (Fig. 4c–e) secondary $Cr_{23}C_6$ carbides form even precipitates in spaces among primary carbides. The borides present in these alloys undergo fragmentation and dissolution (Fig. 5a and b).

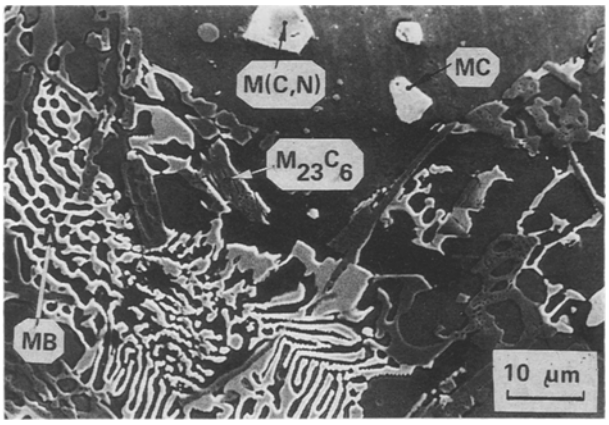

Figure 2 SEM micrograph of alloy no. 4, as-cast condition. Etch 50% HNO_3, electrolytic.

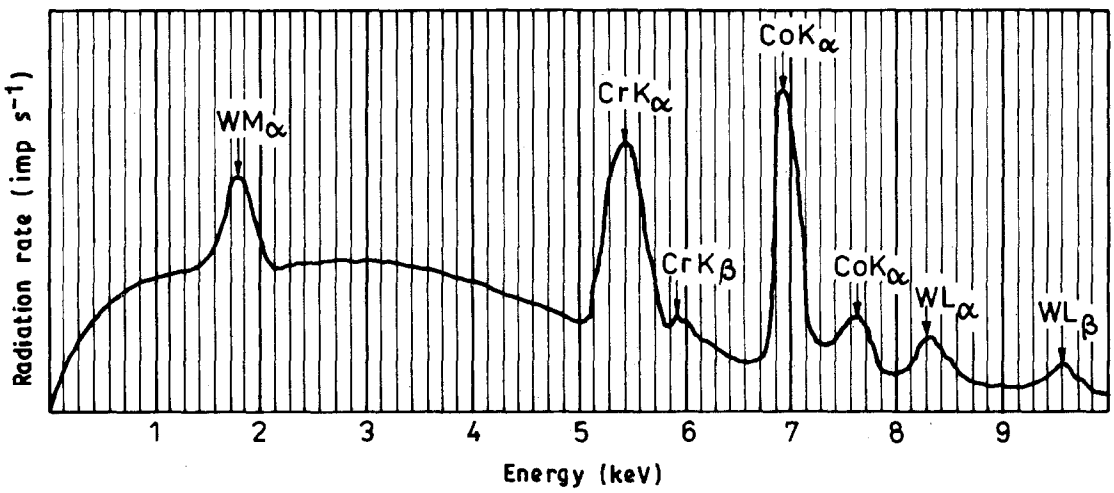

Figure 3 Characteristic radiation spectrum for boride phase, observed on the spectrometer monitor "Kevex-Ray"

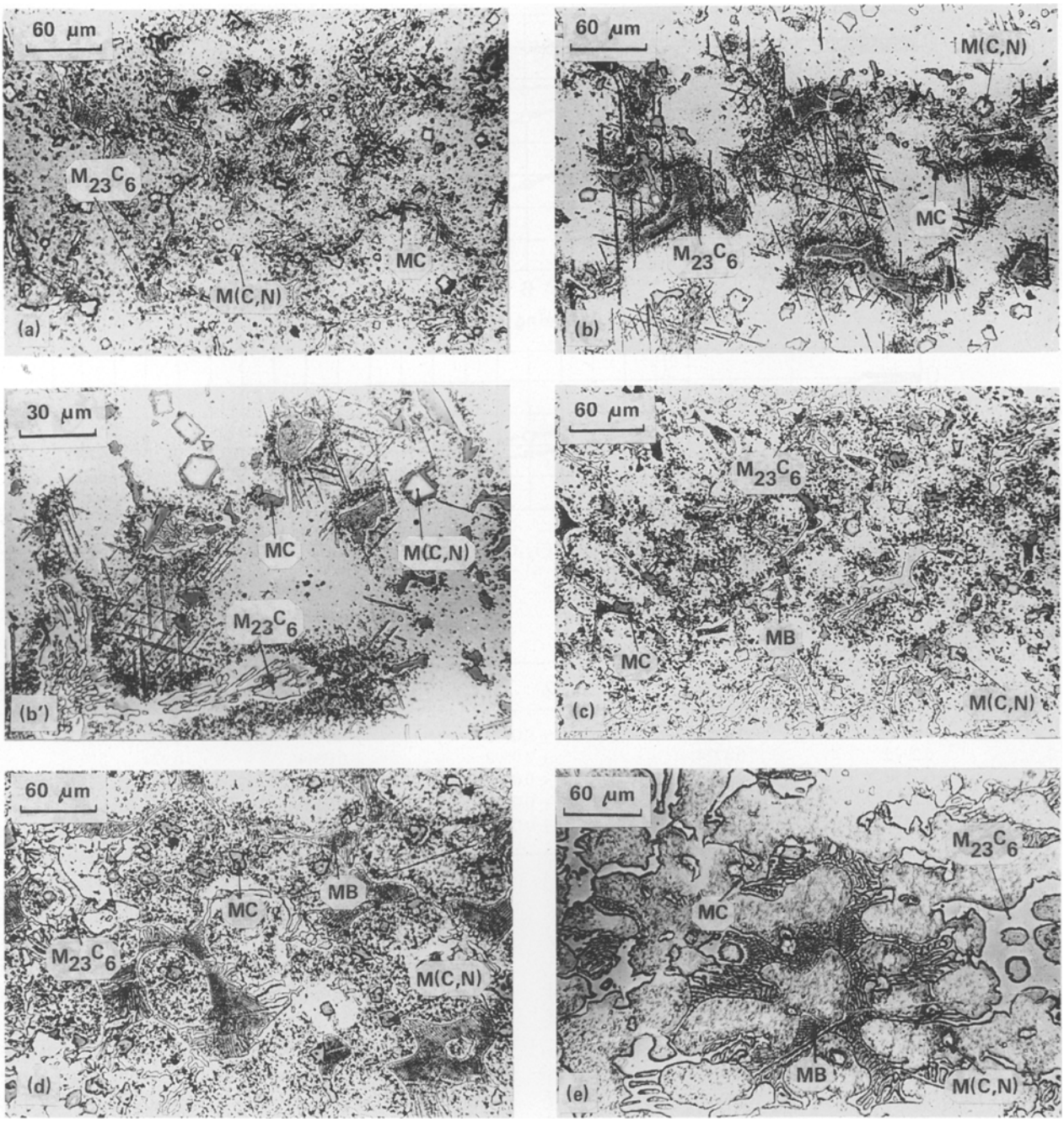

Figure 4 As-cast condition and after ageing at 975 °C for 21 h of MAR–M509 type alloys. Etch 50% HNO_3, electrolytic. Alloy no. (a) 1, (b, b') 2, (c) 3, (d) 4, (e) 5.

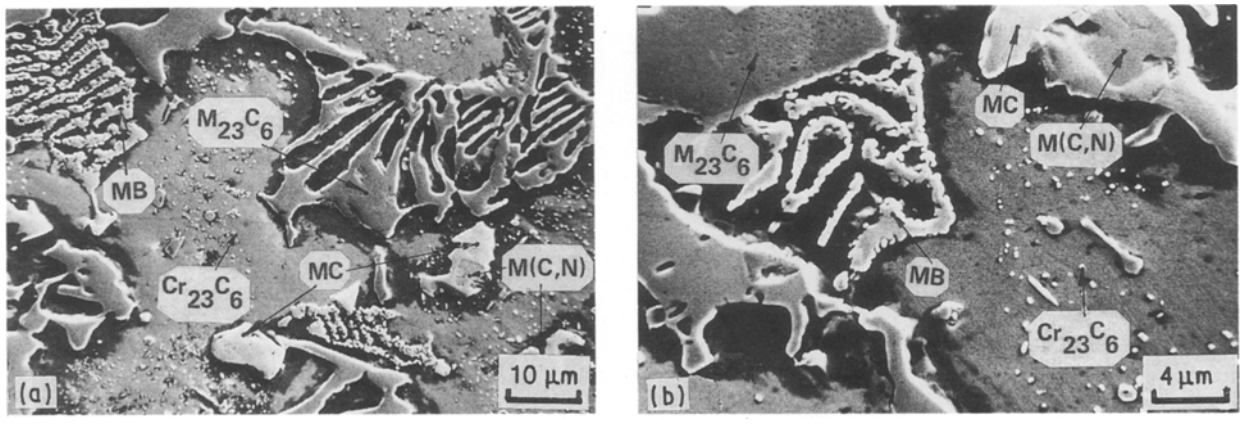

Figure 5 SEM micrograph of alloy no. 5, as-cast condition and after annealing at 975 °C for 21 h. Etch 50% HNO_3, electrolytic.

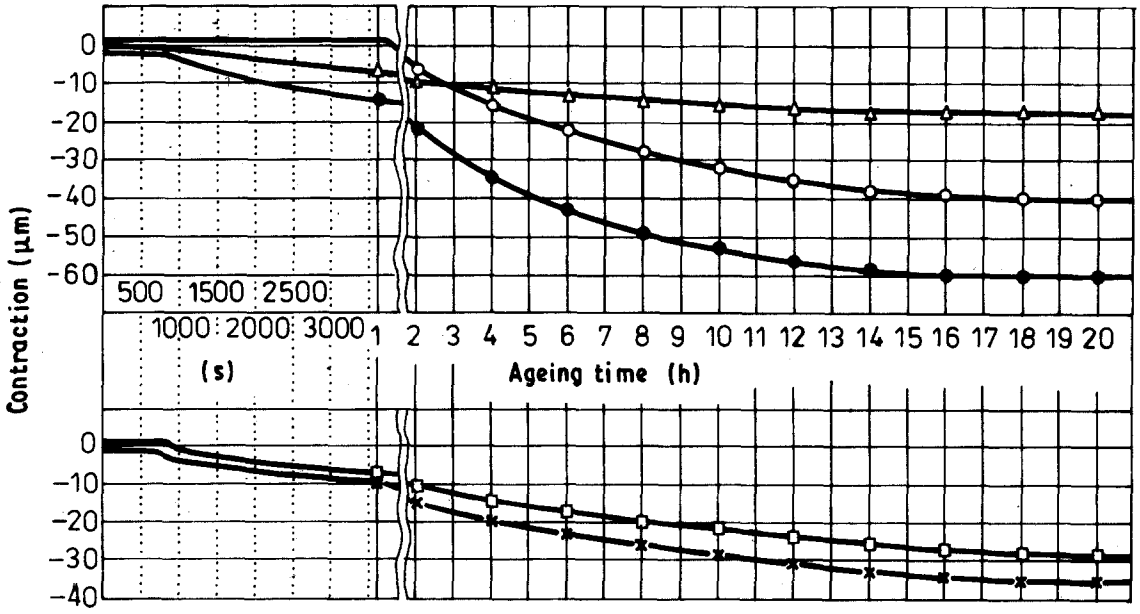

Figure 6 Dilatometer curves of precipitation kinetics of secondary $Cr_{23}C_6$ carbides. Alloy no. ○, 1; △, 2; ●, 3; □, 4; ×, 5. Annealing (ageing) temperature of alloys at 975 °C.

TABLE II Values for alloys 1 to 5 annealed at 975 °C for 21 h

Alloy no.	k	n	D_n	D_k	c.c.
1	0.0515	1.0219	± 0.0973	± 0.0096	0.984
2	0.2975	0.4724	± 0.0592	± 0.0544	0.974
3	0.2554	0.4498	± 0.0605	± 0.0593	0.965
4	0.2462	0.4437	± 0.0331	± 0.0349	0.986
5	0.2475	0.4626	± 0.0345	± 0.0362	0.986

3.2. The precipitation kinetics of secondary $Cr_{23}C_6$ carbides

The dilatometer LS-4 was used for the precipitation of secondary $Cr_{23}C_6$ carbides in cobalt austenite γ of heat-resistant casting alloys of the MAR-M509 type, modified by boron additions. The dilatometer curves of precipitation kinetics in alloys 1 to 5, $t = f$ (Specimen contraction), are shown in Fig. 6. All the specimens were isothermally annealed at 975 °C for 21 h. The alloys were heated together with the dilatometer furnace to about 975 °C at about 450 °C h^{-1} and then isothermally annealed. Dilatometer curves were registered on the paper tape with the indicating speed of 20 mm h^{-1}.

Dilatometer kinetics curves of secondary $Cr_{23}C_6$ carbide precipitation in the investigated cobalt alloys are described by Wert's equation [12]:

$$W_t = kt^n \quad (1)$$

where W_t is the degree of transformation (determined from the dilatometer curve) at annealing time t (0–21 h), and k and n are constants.

The equation constants were computed using a ZX Spectrum microcomputer, by linear regression, using Basic. Therefore the equation assumed the following form:

$$\log W = n \log t + \log k \quad (2)$$

introducing $\log k = \ln k / \ln 10$ ($\ln 10 = 2.302585$).

Using Student's t-test the following values were assumed: confidence level = 0.95, significance coefficient $\alpha = 0.05$, and for the 21 independent variables (time of alloy annealing = 21 h) coefficient value = 2.080.

Constants k and n, constants of standard deviations (s.d.) D_n, D_k and correlation coefficient (c.c.) were defined from the calculations. Their values are listed in Table II.

4. Conclusions

The influence of boron addition to cobalt-base casting alloys of the MAR-M509 type on the precipitation kinetics of secondary $Cr_{23}C_6$ carbides in their matrices at 975 °C is presented. Kinetics investigations were extended by the examination of the microstructure of alloys in the as-cast condition and after isothermal annealing. It was found that the addition of boron of about 0.09% (alloy no. 2) does not lead to the separation of new boride phases, but to the size reduction of primary carbide and carbonitride phases. However, after annealing it promotes an uneven precipitation of the secondary $Cr_{23}C_6$ carbides in the alloy matrix. This level of boron (0.09%) is probably very close to the solubility limit of this element in the solid solution γ. It can be concluded from the distribution characteristics of the secondary $Cr_{23}C_6$ carbides that boron helps their precipitation to occur around the primary $M_{23}C_6$ carbides with high chromium content.

0.47% B content in alloy no. 3 considerably exceeds the solubility limit. The MB-type borides are formed with a high tungsten content, which is present in the solid solution γ. The borides precipitated in alloys 3 to 5 are complex and can be determined as (W, Cr, Co) B. In alloy no. 3 they are precipitated as separate concentrated phases and in alloys 4 and 5 they are eutectically crystallized together with the carbides of the $M_{23}C_6$ type. In alloys 3 to 5 the crystallized borides promote the creation of a continuous net of primary carbides around the grains of solid solution γ, and the secondary $Cr_{23}C_6$ carbides are evenly precipitated in the matrix.

In all alloys that contain boron (alloys 2 to 5) this element significantly reduces the incubation time for $Cr_{23}C_6$ carbide nucleation from about 3780 s for alloy no. 1 (with no boron content) to about 680 s for alloy no. 5 (with 1.48% B content). Moreover, boron dissolved in the matrix of alloy no. 2 in the as-cast condition near its solubility limit, causes a supersaturated solution. This was demonstrated by a great contraction of the specimen (about 60 μm) after annealing at 975 °C for 21 h. The precipitation of boride phases decreases the degree of solutioning as the contraction of the specimen is smaller.

The precipitation kinetics of secondary $Cr_{23}C_6$ carbides in the analysed cobalt-base alloys are well described by Wert's equation. The correlation coefficients (c.c.) approximate to 1.0. The kinetics of secondary $Cr_{23}C_6$ carbide precipitation for cobalt alloys of the MAR–M509 type with no boron content, during annealing at 975 °C for 0 to 21 h may be described by the following:

$$W_t = 0.05t^{1.02}$$

In Wert's equation, boron additions clearly change contents k and n in comparison with alloy no. 1 (with no boron content). The equation of the precipitation kinetics of secondary $Cr_{23}C_6$ carbides in alloys of the MAR–M509 type containing about 0.1% B dissolved in matrix γ assumes the following form:

$$W_t = 0.3t^{0.47}$$

and for the alloys containing more boron (above 0.1% B) when the primary borides of the MB type are precipitated, the equation is:

$$W_t = 0.25t^{0.45}$$

References

1. R. STICKLER, in "High-Temperature Materials in Gas Turbines", edited by P. R. Sahm and M. O. Speidel (Elsevier Scientific, Amsterdam-London-New York, 1974) p. 115.
2. Z. OPIEKUN, *J. Mater. Sci.* **22** (1987) 1547.
3. J. B. VANDER SANDE, J. R. COKE and J. WULFF, *Metall. Trans.* **7A** (1976) 389.
4. A. J. T. CLEMOW and B. L. DANIELL, *K. Biomed. Mater. Res.* **13** (1979) 265.
5. R. N. J. TAYLOR and R. B. WATERHOUSE, *J. Mater. Sci.* **18** (1983) 3265.
6. H. S. DOBBS and J. L. M. ROBERTSON, *ibid.* **18** (1983) 391.
7. R. N. J. TAYLOR and R. B. WATERHOUSE, *ibid.* **21** (1986) 1990.
8. T. KILNER, A. J. DEMPSEY, R. M. PILLIAR and G. C. WEATHERLY, *ibid.* **22** (1987) 565.
9. L. ZHUANG and EBBE W. LANGER, *Z. Metallkde. Bd.* **80** (1989) 251.
10. UK Patent No. 1376479 (1972).
11. K. DZIEDZIC, PhD thesis, Politechnika Šlaska–Wydz. Metalurgiczny (1985) Katowice, ul Craniczna 1, Poland.
12. C. WERT, *J. Appl. Phys.* **21** (1950) 1.

Received 27 February
and accepted 6 June 1990